Solvation dynamics of molecular glass-forming liquids in confinement

2003 J. Phys.: Condens. Matter 15 S1041

(http://iopscience.iop.org/0953-8984/15/11/326)

INSTITUTE OF PHYSICS PUBLISHING JOURNAL OF PHYSICS: CONDENSED MATTER

J. Phys.: Condens. Matter **15** (2003) S1041–S1050 PII: S0953-8984(03)58214-5

Solvation dynamics of molecular glass-forming liquids in confinement

Ranko Richert and Min Yang

Department of Chemistry and Biochemistry, Arizona State University, Tempe, AZ 85287-1604, USA

Received 14 October 2002
Published 10 March 2003
Online at stacks.iop.org/JPhysCM/15/S1041

Abstract

Triplet state solvation dynamics experiments on geometrically confined glass-forming liquids are performed in order to study the effects of confinement on length scales of several nanometres. Variations of the surface chemistry of porous glasses and the spatially selective observation of the interfacial liquid layer indicate that the surface interactions determine the difference between the dynamics of the bulk and confined situations. For 3-methylpentane in pores of 7.5 nm diameter, the timescale of interfacial dynamics is slowed down by three orders of magnitude, while structural relaxation already remains bulk-like just a few nanometres away from the silica surface. The time-resolved optical linewidths indicate dynamical heterogeneity in confined liquids, but the signature differs from the bulk case.

1. Introduction

Materials alter their properties if their spatial extent is changed from the bulk to a few nanometres. Such confinement effects are interesting as regards both technological and fundamental aspects. During the last decade, glass-forming materials have been the subject of numerous studies concerned with the influence of restricting geometries [1–3]. Such supercooled liquids are characterized by complex dynamics in terms of non-exponential correlation functions and non-Arrhenius temperature dependences of the average structural relaxation time [4]. At the glass transition temperature T_g the relaxation timescale reaches a value of $\tau_g = 100$ s, resulting in the non-equilibrium glassy state if the system is cooled further below T_g at typical cooling rates [5]. An important feature of glass-formers is their cooperative nature of the molecular motion, whose increasing length scale $\xi(T)$ is often held responsible for the pronounced slowing down of the dynamics as T approaches T_g [6]. This length scale with $\xi(T_g) \approx 3$ nm can be considered the distance required by two molecules to relax independently.

Jackson and McKenna [7] have conducted a differential scanning calorimetry study of how the glass transition of organic glass-forming materials is affected by confinement to

porous glasses. Their observation of a confinement-induced lowering of T_g by a few kelvins is equivalent to faster dynamics in the pores compared with the bulk if assessed at the same temperature. In the meantime, many different experimental techniques have been applied to supercooled liquids and polymers in order to study confinement effects associated with length scales of several nanometres [8–13]. Glass transition shifts ΔT_g of up to 70 K have been reported for free-standing amorphous polymer films [14]. In some cases, structural ordering has been held responsible for a significant reduction in the molecular mobility near the surface [15, 16]. The fact that both positive and negative values are being reported for ΔT_g implies that both accelerated as well as frustrated dynamics are being observed in nano-confined materials relative to their bulk counterparts [17]. Additionally, ΔT_g reflects only a change in the average timescale of the dynamics, and substantial variations of the correlation functions remain obscured if finite-size and interfacial effects are reduced to ΔT_g.

Porous silica glasses obtained from sol–gel processes or spinodal decomposition exhibit irregular internal structures and a distribution of surface curvatures, similarly to natural porous materials [18]. Optically transparent porous silica is readily available with average pore sizes as small as 2.5 nm, yielding ideal samples for triplet state solvation dynamics experiments on molecular glass-formers subject to geometrical confinement. In this work, we compile several results obtained from solvation dynamics measurements in order to address the importance of surface compared with finite-size effects. The results are discussed in the context of cooperative motion and dynamic heterogeneity.

2. Experiments

Solvation dynamics experiments require the long-lived excited triplet states for assessing the sluggish dynamics of molecules in the supercooled state close to the glass transition at T_g [19]. The method rests upon the electronic excitation of a chromophore as a dopant whose permanent dipole moment changes from the ground state value μ_G to that of the excited state μ_E. The time-resolved $S_0 \leftarrow T_1(0\text{–}0)$ emission spectrum exhibits a shift towards lower energies whenever dielectric polarization is active within the phosphorescence lifetime τ_{ph}. The Stokes shift dynamics of the average emission energy thus reflects the orientational polarization of dipolar solvents [20]. In the case of non-polar systems, the solvation dynamics reflects the local shear modulus relaxation [21, 22]. This triplet state solvation technique is highly suitable for investigating the relaxation of viscous liquids in porous silica glasses, because the probe molecules are sensitive only to the local response, and the second solvent shell already has little effect on the line shift.

The resulting $S_0 \leftarrow T_1(0\text{–}0)$ emission spectra are subjected to a Gaussian analysis in order to determine the average emission energies $\langle \nu(t, T) \rangle$ and the linewidths $\sigma(t, T)$ as a function of time and temperature. To focus on the dynamical aspect of the dipolar solvation process at a fixed temperature, the $\langle \nu(t) \rangle$ data are normalized according to the Stokes shift correlation function

$$C(t) = \frac{\langle \nu(t) \rangle - \langle \nu(\infty) \rangle}{\langle \nu(0) \rangle - \langle \nu(\infty) \rangle}. \tag{1}$$

The total Stokes shift $\Delta = \langle \nu(0) \rangle - \langle \nu(\infty) \rangle$ is a measure of the amplitude of the response, whereas the signal intensities remain irrelevant for the data analysis. In many cases, the correlation decays $C(t)$ are well approximated by a stretched exponential or Kohlrausch–Williams–Watts (KWW) function of the form

$$C(t) = \exp[-(t/\tau_{KWW})^{\beta}], \tag{2}$$

with a temperature-invariant exponent β in the present temperature ranges. Thus, temperature variations affect $C(t)$ only in terms of the characteristic time $\tau_{KWW}(T)$ without changing the functional form. The time-resolved Gaussian width $\sigma(t)$ is the relevant quantity for assessing the heterogeneous nature of the dynamics [23].

Most porous glasses used here are Gelsil glasses (from GelTech) of cylindrical shape (10 mm ϕ, 5 mm thick) with nominal pore diameters $\phi = 2.5$, 5.0, and 7.5 nm. Based on N_2-BET adsorption isotherm results supplied by GelTech, the actual characteristics in the above order of ϕ are: pore diameters: 2.6, 4.6, and 8.4 nm; pore volume fractions: 0.39, 0.68, and 0.72; and surface areas: 609, 594, and 342 $m^2\ g^{-1}$. To a good approximation, the pore size distributions are Gaussians with widths $\sigma \approx 0.15\ \phi$. One sample employed porous Vycor glass (Corning) with a pore size of 2.7 nm. Clean pore surfaces are obtained by washing with isopropanol and 30% H_2O_2 and heating in vacuum for 24 h. Silanized glasses have been prepared by exposing the dried porous glass to hexamethyldisilazane gas at ambient temperatures for 24 h. The glasses were filled with the solute/solvent mixture under dry N_2 atmosphere and placed into a vacuum-sealed sample cell.

Two different probe molecules at concentrations of 2×10^{-4} mol mol^{-1} have been used in these studies. Quinoxaline (QX) with a triplet lifetime $\tau_{ph} = 0.3$ s undergoes a significant change in dipole moment, $\mu_E - \mu_G = 1.3$ D, and thus couples to dipolar relaxations in the solvent. Naphthalene (NA) exhibits a triplet lifetime of $\tau_{ph} = 2.2$ s and lacks a change in dipole moment, $\mu_E \approx \mu_G$. Therefore, the solvation of NA is purely mechanical and reflects the shear modulus of the surrounding solvent. The glass-forming liquids of this study are 2-methyltetrahydrofuran (MTHF), a moderately polar liquid with $T_g = 91$ K, and 3-methylpentane (3MP), a non-polar liquid with $T_g = 77$ K. Because 3MP is not associated with any significant dipole moment, the solvation of both QX and NA in 3MP originates from the local time-dependent shear modulus.

3. Results and discussion

Solvation dynamics $C(t)$ results for the solute QX in the glass-forming solvent MTHF have been obtained from porous glass samples subjected to different surface treatments [12, 24]. In the case of silanized surfaces, the silanol groups of a native silica surface are passivated, which leads to more hydrophobic pore walls. For this case, panel (A) of figure 1 shows that the dynamics of MTHF remains unchanged compared with the bulk situation, even in the smallest pores of 2.5 nm diameter. This demonstrates that finite sizes of a few nanometres do not necessarily lead to different dynamics in viscous liquids. For the clean but otherwise untreated and more hydrophilic pore boundary case of panel (B) of figure 1, the situation is entirely different. Here, confinement does affect the dynamics significantly in the longer time range, while the short-time relaxation remains that of the bulk case. Because these two examples of confinement effects differ only in the liquid/solid interactions at the surface, the chemical and physical properties of the boundary are considered crucial for the understanding of geometrical restrictions. The additional very slow relaxation component observed for the native glass surface gains relative amplitude as the pore size or temperature is decreased. Our original [12] interpretation assumed that the slow dynamics is associated with molecules near the interface and that temperature determines the length scale ξ of cooperativity [6], which controls the extent to which the surface-induced frustration penetrates into the pore volume. This interpretation is supported by the similarity of the bimodal correlation decays in panel (B) of figure 1 to the results obtained from simulation work on the dynamics in a confined model system [25]. However, the above experiments are not decisive regarding a specific spatial position of the slowly relaxing modes.

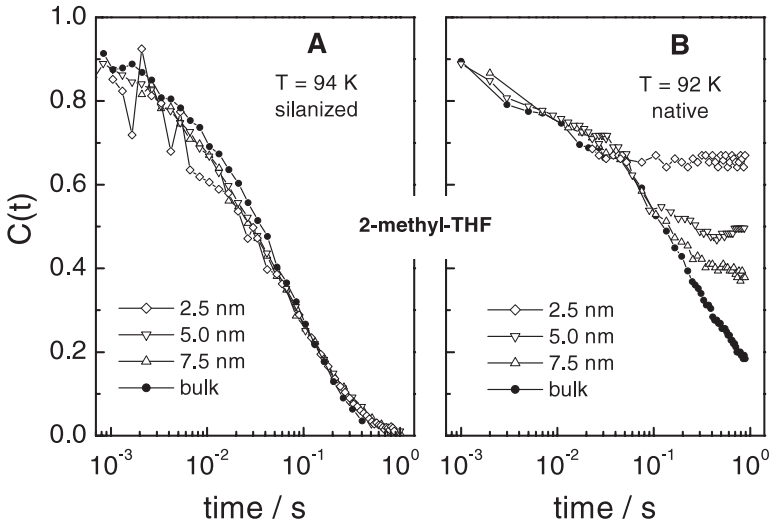

Figure 1. Stokes shift correlation function $C(t)$ versus time for QX/MTHF in the bulk and confined to various pore sizes as indicated. (A) Results for a silanized glass surface, which leads to a hydrophobic interface. (B) Results for a clean but otherwise untreated glass surface.

A deeper insight into the dependence of the liquid dynamics on the distance from the pore wall requires a spatially resolved measurement. As we realized previously, solvation techniques offer spatial selectivity achievable by attaching the probe molecules to the surface of a porous glass [24]. The initial solvation measurement using surface-bound probes lacked time resolution and therefore remained ambiguous regarding the relaxation behaviour at the interface. However, we have recently succeeded in recording the solvation dynamics of QX as a surface probe in the liquid 3MP [26]. The absolute emission energy of the QX in 3MP-filled porous glass reveals that all probes are bound to the silanol groups of the silica surface. Under otherwise identical conditions, the dynamics within the pore volume can be probed using NA as a chromophore, which remains in solution.

The resulting relaxation timescales for bulk, confined, and interfacial 3MP in porous glasses of 7.5 nm pore diameter are compiled in figure 2. The three sets of correlation decays are well described by the KWW-type decay of equation (2), and severe timescale separations like those observed for confined MTHF remained absent in 3MP. The solid curves in figure 2 are Vogel–Fulcher–Tammann (VFT) fits to the temperature dependence $\tau_{KWW}(T)$ according to

$$\log_{10}(\tau_{KWW}/\mathrm{s}) = A + B/(T - T_0). \tag{3}$$

The activation parameter $B = 464$ K and divergence temperature $T_0 = 52$ K are common to all three data sets, while $A_{bulk} = -16.8$, $A_{conf} = -15.2$, and $A_{intf} = -13.5$ is found for the bulk, confined, and interfacial cases, respectively. On the basis of the $\tau(T_g) = 100$ s criterion for identifying T_g, we find $T_{g,bulk} = 76.7$ K for the bulk liquid, $\Delta T_{g,conf} = +2.3$ K for 3MP confined to the 7.5 nm pores, and $\Delta T_{g,intf} = +5.2$ K for the interfacial 3MP. At a given temperature, comparing the average timescale within the pore with that in the bulk leads to $\tau_{conf}/\tau_{bulk} = 40$, whereas the relaxation time within the interfacial layer is slower by a factor of $\tau_{intf}/\tau_{bulk} = 2000$. Accordingly, the viscosity η of the interfacial layer is around three orders of magnitude larger than that of the bulk liquid.

The dynamics observed in bulk 3MP is independent of the solute used, NA or QX, and in both cases the $C(t)$ traces are consistent with a KWW exponent $\beta_{bulk} = 0.42$. For the

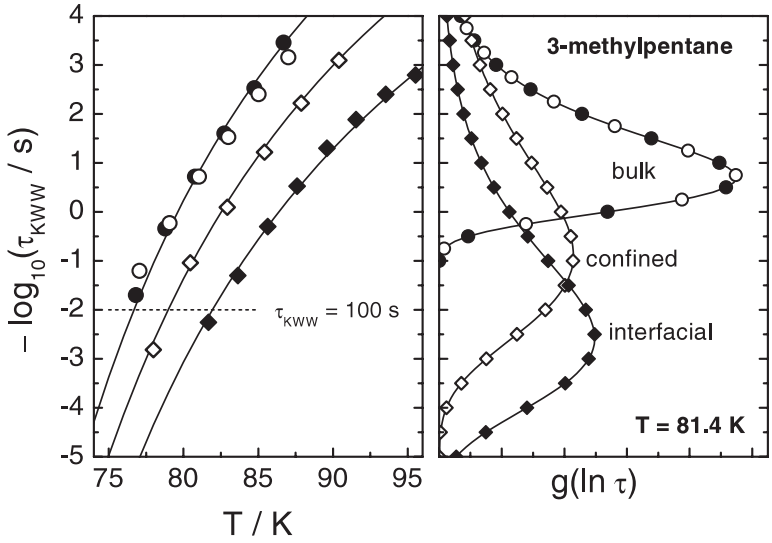

Figure 2. The temperature dependence of the solvent relaxation time in 3MP for the bulk liquid (QX/3MP: solid circles; NA/3MP: open circles), for 3MP confined to 7.5 nm pores (NA/3MP: open diamonds), and for the interfacial layer of 3MP at the pore wall (QX/3MP: solid diamonds). The solid curves are VFT fits; the dotted curve indicates the $\tau = 100$ s criterion for determining T_g. The probability densities $g(\ln\tau)$ of relaxation times τ are shown for $T = 81.4$ K in the rhs panel using the same ordinate scale. The curves are for the bulk liquid ($\beta = 0.42$), for 3MP confined to 7.5 nm pores ($\beta = 0.22$), and for the interfacial layer of 3MP at the pore wall ($\beta = 0.25$).

average over the pore volume we find $\beta_{conf} = 0.22$, while the interfacial case is characterized by $\beta_{intf} = 0.25$. The probability densities $g(\ln\tau) = \tau g(\tau)$ based upon the values of β and τ for the bulk, confined, and interfacial situations are shown for $T = 81.4$ K in the rhs panel of figure 2. Observing that much of the $g(\ln\tau)$ area for the confined case overlaps with the range of τ-values observed in the bulk suggests that a fraction of the liquid within the pore behaves in a bulk-like manner; this most probably arises from the pore centre. This notion justifies the tentative trend of relative relaxation times as a function of the distance r ($0 \leqslant r \leqslant R$) from the centre: $\tau(r = 0) = \tau_{bulk}$, $\tau(r = \langle r\rangle = R/4) = \tau_{conf} = 40 \times \tau_{bulk}$, and $\tau(r = R) = \tau_{intf} = 2000 \times \tau_{bulk}$, i.e., at the interface. The resulting $\tau(r)$ trace is displayed in figure 3 and resembles the spatially resolved dynamics derived from MD simulations of a confined 80:20 binary Lennard-Jones liquid [27]. This distance dependence is consistent with a length scale ξ for cooperative motion of 2–3 nm near T_g, i.e. only molecules at a distance of a few nanometres are capable of relaxing independently of the condition at the pore boundary.

Given this pronounced gradient of relaxation times within 7.5 nm pores, one wonders what the behaviour of the liquid will be at even smaller pore sizes. Our preliminary assessment of more severe geometrical restrictions is based upon the pore-averaged dynamics obtained using NA in 3MP confined to 5.0 nm pores, and the interfacial dynamics of 3MP probed by QX bound to the surface of a Vycor glass with 2.7 nm pore size. The results in terms of $\tau_{KWW}(T)$ are displayed in figure 4, which includes the 7.5 nm data of figure 2 for comparison. In these smaller pores, only a minor difference remains between the pore-volume-averaged and interfacial dynamics. For temperatures in excess of 90 K, the curves coincide with the interfacial timescales derived for the 7.5 nm sample. However, the previous VFT-type curvature of $\tau_{KWW}(T)$ is lost and the smaller pore sizes give rise to more Arrhenius-like behaviour with a concomitant return of T_g towards the bulk value. A possible explanation for losing the super-

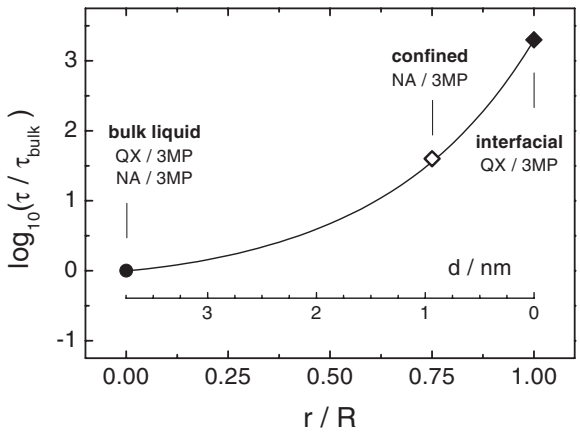

Figure 3. The suggested trend for $\tau(r)/\tau_{bulk}$ based upon $\tau_{bulk}/\tau_{bulk} = 1$ for $r = 0$ (QX and NA in bulk 3MP), $\tau_{conf}/\tau_{bulk} = 40$ for $r = \langle r \rangle \approx R/4 = 0.94$ nm (NA/3MP in pores), and $\tau_{intf}/\tau_{bulk} = 2000$ for $r = R = 3.75$ nm (QX/3MP in pores). The curve is an empirical interpolation only. The inner scale shows the distance d from the interface for a spherical geometry.

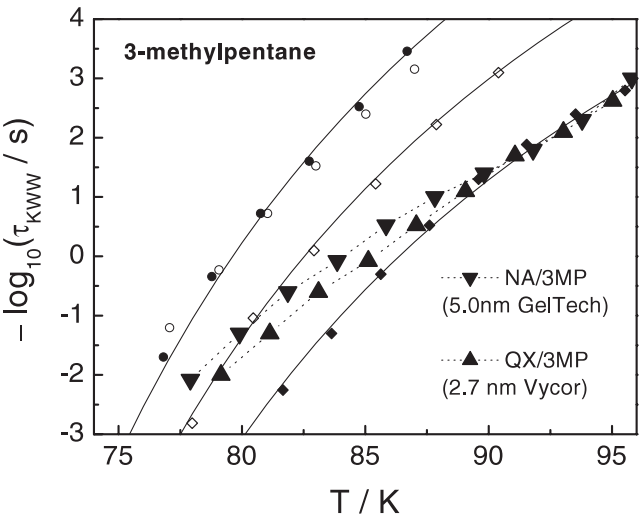

Figure 4. The temperature dependence of the solvent relaxation time in 3MP for a confinement to 5.0 nm pores (NA/3MP: downward-pointing triangles), and for the interfacial layer of 3MP at the pore wall (QX/3MP: upward-pointing triangles) of porous Vycor with 2.7 nm pore size. The solid curves and small symbols repeat the data of figure 2 for comparison.

Arrhenius behaviour is that the thermodynamic conditions of constant pressure no longer apply, because material flow is sufficiently impeded within the bottlenecks which interconnect the pores. On the other hand, there are systems where this effect sets in only at temperatures just below the bulk glass transition [28].

A further length scale inherent in the structural relaxation of glass-forming liquids is that associated with dynamic heterogeneity [29, 30]. This heterogeneity in an otherwise homogeneous liquid refers to the property of relaxation times being spatially varying quantities, i.e. slow and fast dynamics are clustered in real space [31, 32]. In solvation dynamics

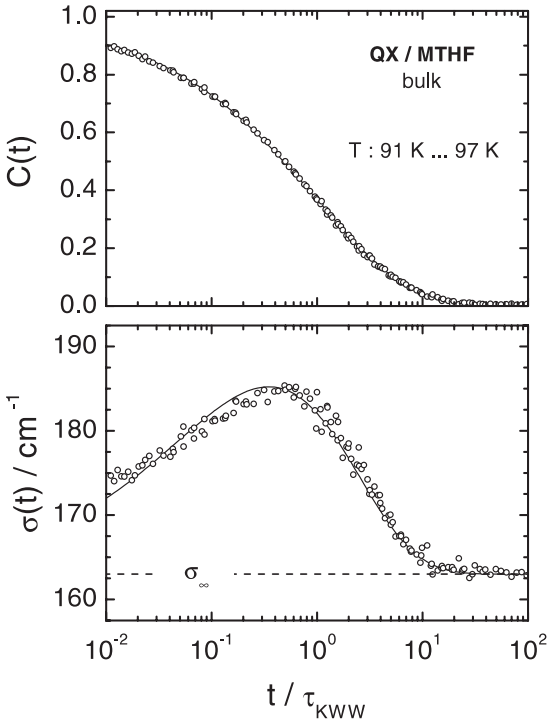

Figure 5. A master plot of the Stokes shift correlation function $C(t)$ (symbols, top) and of the inhomogeneous linewidth $\sigma(t)$ (symbols, bottom) versus t/τ_{KWW} for the solute QX in the solvent MTHF, measured at temperatures in the range 91 K $\leqslant T \leqslant$ 97 K in steps of 1 K. The solid curve in the top panel is a fit to $C(t)$ using a stretched exponential, $C(t) = \exp[-(t/\tau_{KWW})^{0.5}]$. The solid curve in the bottom panel is based upon a static distribution of intrinsically exponential responses, whereas homogeneity would lead to $\sigma(t) \equiv \sigma_\infty$.

experiments, the signature of heterogeneity is a peak in the time-resolved linewidth $\sigma(t)$ [23], which remains unexplained within models of homogeneous solvent dynamics [33, 34]. A particularly well resolved solvation measurement is that of QX in bulk MTHF, where the initial (σ_0) and steady-state (σ_∞) linewidths happen to be the same [35]. In the case of $\sigma_0 = \sigma_\infty$ and assuming a static distribution of exponential local response functions, the following equation (4) relates $\sigma(t)$ to $C(t)$ with no adjustable parameter, because σ_∞ and Δ can be determined independently [36]:

$$\sigma^2(t) = \sigma_\infty^2 + \Delta^2[C(2t) - C^2(t)]. \tag{4}$$

Figure 5 shows $C(t)$ and $\sigma(t)$ for the QX/MTHF sample together with the prediction given by equation (4). Note that $\sigma(t) \equiv \sigma_\infty$ would be expected on the basis of a homogeneous model of solvent dynamics.

Now, recall that the solvation dynamics of QX/MTHF has remained practically identical for the bulk liquid and for the case of confinement to porous glasses with a silanized silica surface (see panel (A) of figure 1). Therefore, it is interesting to examine whether the signature of heterogeneity is also finite-size invariant. The solvent shift in the bulk is characterized by $\Delta = 246\ \text{cm}^{-1}$ and $\beta = 0.50$, and the data obtained from the same system in 5.0 nm pores lead to very similar values, $\Delta = 232\ \text{cm}^{-1}$ and $\beta = 0.47$. Additionally, the temperature dependence of the mean relaxation times is virtually unaffected by confinement to silanized pores [37]. Figure 6 repeats the analysis of figure 5 for silanized pores of 5.0 nm diameter, again

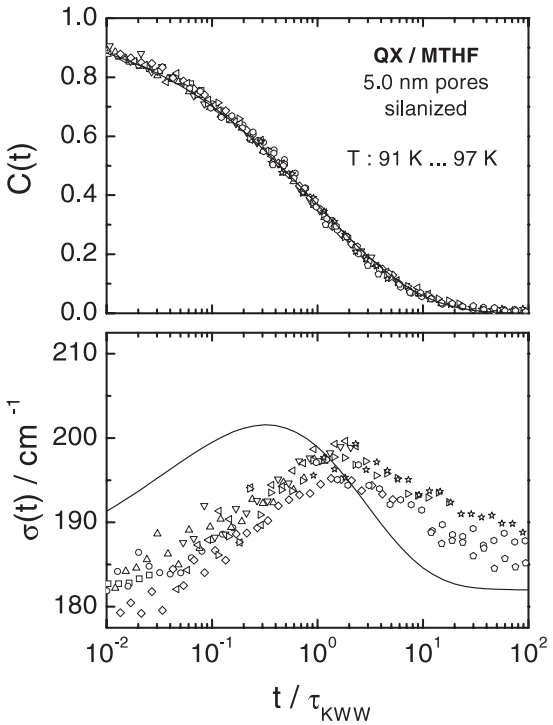

Figure 6. As figure 5, but for QX/MTHF in silanized porous glass with 5.0 nm average pore diameter.

showing the data for different temperatures (91 K $\leqslant T \leqslant$ 97 K) on a master timescale using t/τ_{KWW} instead of t. Although the $C(t)$ suggests dynamics which are identical to the bulk case, the time-resolved linewidth $\sigma(t)$ differs considerably from what is expected on the basis of equation (4). Although the peak of $\sigma(t)$ in figure 6 clearly indicates heterogeneity regarding the solvent dynamics, its occurrence appears retarded on the timescale relative to $C(t)$. Although an explanation for the impact of confinement on $\sigma(t)$ cannot be offered at present, the linewidth is likely to reveal subtle effects to which the average energy or $C(t)$ is not as sensitive. In any case, a closer scrutiny of optical lineshapes in geometrically confined solvent might shed light on how dynamic heterogeneity is affected by boundary or finite-size effects.

4. Concluding remarks

Triplet state solvation dynamics experiments are employed for assessing the effects of confinement on the dynamics of molecular glass-forming liquids. Because the observed correlation functions are independent of the signal intensity and only the nearest-neighbour dynamics is probed, this technique is an appropriate tool for studying liquids confined to porous glasses and the data interpretation is straightforward. Additionally, the response amplitudes are unambiguously resolved, which is an important requirement for comparing bulk and confined correlation functions. A very powerful option of this method is the capability of binding probe molecules to the confining surface, which enables us to look into the dependence of the dynamics on the distance from the pore boundary.

As has been demonstrated by varying the surface chemistry and more convincingly by selectively probing the surface layer of the liquid, the interactions of the liquid constituents

with the pore surface play a vital role in defining the confinement effects. Therefore, not only surface chemistry but also curvatures and roughness on the molecular level will be important for predicting how confinement alters the dynamics and structure of a supercooled liquid. The experimental results outlined above do not support any obvious finite-size effects. Instead, the observed features can be rationalized on the basis of possibly frustrated interfacial dynamics, with the length scale of cooperative motion being responsible for the spatial range over which these slower relaxation times extend into the pore volume. Additionally, the heterogeneous nature of the dynamics can be confirmed also in pores of 5 nm diameter, but the time-resolved linewidth used to infer heterogeneity differs significantly from the bulk counterpart. It appears interesting to further explore the origin of these unexpected optical lineshapes in the situation of geometric restrictions.

The spatial range of confinement employed in this study, 2.5–7.5 nm, is particularly interesting because pore sizes of a few nanometres are comparable to two important (but perhaps related) length scales inherent in the dynamics of viscous materials, that of cooperativity and that associated with dynamical heterogeneity. Because the developments of these lengths are being restricted in nm-sized pores, experiments on such systems will provide critical tests of our understanding of cooperativity, heterogeneity, and the details of interactions at the interface on a molecular level. Therefore, advances in this field will not only lead to an improved picture of confinement effects, but at the same time supply valuable information which helps in rationalizing the behaviour of bulk materials on a microscopic scale.

References

[1] Drake J M and Klafter J (ed) 1989 *Molecular Dynamics in Restricted Geometries* (New York: Wiley)
[2] Drake J M, Grest G S, Klafter J and Kopelman R (ed) 1999 *Dynamics in Small Confining Systems* vol 4 (Pittsburgh, PA: Materials Research Society)
[3] Frick B, Zorn R and Büttner H (ed) 2000 *J. Physique* IV **10**
[4] Ediger M D, Angell C A and Nagel S R 1996 *J. Phys. Chem.* **100** 13200
[5] Angell C A, Ngai K L, McKenna G B, McMillan P F and Martin S W 2000 *J. Appl. Phys.* **88** 3113
[6] Adam G and Gibbs J H 1965 *J. Chem. Phys.* **43** 139
[7] Jackson C L and McKenna G B 1991 *J. Non-Cryst. Solids* **131–133** 221
[8] Zhang J, Liu G and Jonas J 1992 *J. Phys. Chem.* **96** 3478
[9] Huwe A, Kremer F, Behrens P and Schweiger W 1999 *Phys. Rev. Lett.* **82** 2338
[10] Schüller J, Mel'nichenko Y B, Richert R and Fischer E W 1994 *Phys. Rev. Lett.* **73** 2224
[11] Barut G, Pissis P, Pelster R and Nimtz G 1998 *Phys. Rev. Lett.* **80** 3543
[12] Streck C, Mel'nichenko Y B and Richert R 1996 *Phys. Rev.* B **53** 5341
[13] Loughnane B J, Farrer R A, Scodinu A, Reilly T and Fourkas J T 2000 *J. Phys. Chem.* B **104** 5421
[14] Forrest J A, Dalnoki-Veress K, Stevens J R and Dutcher J R 1996 *Phys. Rev. Lett.* **77** 2002
[15] Cristofolini L, Arisi S and Fontana M P 2000 *Phys. Rev. Lett.* **85** 4912
[16] Cristofolini L, Fontana M P, Berzina T and Konovalov O 2002 *Phys. Rev.* E **66** 041801
[17] McKenna G B 2000 *J. Physique* IV **10** 53
[18] Drake J M and Klafter J 1990 *Phys. Today* **43** 46
[19] Richert R 2000 *J. Chem. Phys.* **113** 8404
[20] Richert R and Wagener A 1991 *J. Phys. Chem.* **95** 10115
[21] Berg M 1994 *Chem. Phys. Lett.* **228** 317
[22] Wendt H and Richert R 1998 *J. Phys. Chem.* A **102** 5775
[23] Richert R 1997 *J. Phys. Chem.* B **101** 6323
[24] Wendt H and Richert R 1999 *J. Phys.: Condens. Matter* **11** A199
[25] Donati C and Jäckle J 1996 *J. Phys.: Condens. Matter* **8** 2733
[26] Richert R and Yang M 2003 *J. Phys. Chem.* B **107** 895
[27] Scheidler P, Kob W and Binder K 2000 *Europhys. Lett.* **52** 277
[28] Simon S L, Park J-Y and McKenna G B 2002 *Eur. Phys. J.* E **8** 209
[29] Schmidt-Rohr K and Spiess H W 1991 *Phys. Rev. Lett.* **66** 3020
[30] Reinsberg S A, Heuer A, Doliwa B, Zimmermann H and Spiess H W 2002 *J. Non-Cryst. Solids* **307–310** 208

[31] Ediger M D 2000 *Annu. Rev. Phys. Chem.* **51** 99
[32] Richert R 2002 *J. Phys.: Condens. Matter* **14** R703
[33] Stephens M D, Saven J G and Skinner J L 1997 *J. Chem. Phys.* **106** 2129
[34] Matyushov D V 2001 *J. Chem. Phys.* **115** 8933
[35] Wendt H and Richert R 2000 *Phys. Rev.* E **61** 1722
[36] Richert R 2001 *J. Chem. Phys.* **114** 7471
Richert R 2001 *J. Chem. Phys.* **115** 1429
[37] Wendt H and Richert R 2000 *J. Physique* IV **10** 67